Appl. Phys. B 66, 145–152 (1998)

Applied Physics B
Lasers
and Optics

Systematic evaluation and prediction of the pulse width of synchronously pumped lasers

U. Morgner[1], **G. Steinmeyer**[2], **F. Mitschke**[3]

[1] Institut für Angewandte Physik, Universität Münster, Corrensstr. 2/4, D-48149 Münster, Germany
(E-mail: morgner@uni-muenster.de)
[2] Department of Electrical Engineering and Computer Science, Massachusetts Institute of Technology, Cambridge, Massachusetts 02139, USA
[3] Fachbereich Physik, Universität Rostock, Universitätsstr. 3, D-18051 Rostock, Germany

Received: 17 March 1997/Revised version: 21 July 1997

Abstract. We reanalyze the pulse width in synchronously pumped lasers. With experimental results from a color center laser, corresponding numerical simulations, and data from the literature, we investigate the dependence of the laser pulse width as a function of the most important parameters without making assumptions about pulse shape stability. We derive an empirical unified fomula that allows us to predict the optimum achieveable pulse width and the required parameter values such as tuner selectivity. It also gives information about pulse properties for other than the optimum choice of parameters. Moreover, it provides information about pulse stability. The formula is also applicable to synchronously pumped optical parametric oscillators.

PACS: 42.60

The generation of tunable ultrashort pulses has relied, through the seventies and eighties, on synchronous pumping of a tunable laser (most often a dye laser) with a train of pulses from a fixed-wavelength pump laser. This useful technique has fallen out of favor with researchers in the nineties because advanced techniques of passive modelocking appear more elegant and allow shorter pulses. Nevertheless, a considerable installed base of synchronously pumped lasers perform in laboratories around the world. Recently, there has been renewed interest in synchronous pumping because passive modelocking is not universally applicable, or practical. Synchronously pumped optical parametric oscillators (OPOs) are a case in point.

In the seventies, theoretical models for the process were worked out. Most of these models, however, assumed self-consistency of the generated pulse. With such an ansatz it is ruled out a priori that the model can predict regimes of unstable pulsing. This was not lost on all researchers: as early as 1970, Pike and Hercher [1] pointed out that the concept of a smooth, periodically repeated pulse shape might be illusory, and argued that possibly the pulses resemble thermal noise within some temporal envelope. In 1979 van Stryland [2] pointed out that in the case of a noisy pulse train the interpretation of autocorrelation signals to deduce the pulse duration could be severely misleading, and that typical observed autocorrelation shapes might be more indicative of noise than of the actual pulse shape. Subsequently, several other authors realized the insufficiency of a self-consistency approach [3–5]. McDonald, Rossel, and Fleming [6] concluded from their experiments that the concept of a noise burst put forward by Pike and Hercher [1] was correct and that the concept of the pulse width as a single quantity was insufficient; rather, they emphasized a strict distinction between the coherence time and the total duration of the pulse.

A large number of experimental and theoretical reports from those years created the impression, however, that a stable regime of operation is always easy to find and that irregularities of the pulse train do not normally occur or do not pose a problem. Such behavior would indeed be hard to detect with standard experimental techniques such as autocorrelation, because these techniques average over many pulses. That does not prove that it does not exist, however, and certainly in some applications such as nonlinear spectroscopy those instabilities would pose severe unexpected and unexplainable problems.

Meanwhile, numerical procedures became more sophisticated, and it became feasible to include realistic fluctuations. In such simulations researchers found instabilities more often than a stable train of pulses [7–10]. New and Catherall went so far as to warn that smooth pulses might actually be impossible to obtain [11].

In the 1990s, new fascinating techniques of passive modelocking were found that have advanced the state of the art considerably. As a side effect, synchronous pumping ceased to be a topic of great current interest. Therefore, many promising lines of research were discontinued at a time when truly realistic concepts were just beginning to emerge. More recently, however, it has been realized that synchronous pumping still has its place in some situations, especially if OPOs are taken into account. Therefore, an unbiased reexamination of the pulse formation process in synchronous pumping is warranted.

Some of the existing knowledge requires close scrutiny. Consider, for example, the output pulse width τ which may be expected to depend, among other things, on the pump pulse duration τ_p. A theoretical result published in 1978 [12, 13]

predicted $\tau \propto (\tau_p)^{1/2}$. This result was tested experimentally by several groups [14–17], and the expected square root dependency was seemingly confirmed. Unfortunately, experiments were restricted to the rather small range of pump pulsewidth variation available at the time. In spite of its independent confirmation and subsequent widespread acceptance, the result was doubted early on [3]. It was shown only recently to be erroneous; even experimental data that supposedly 'confirmed' this relation, make a better fit to a revised theory which has the additional benefit of being more physically intuitive [18].

1 Reexamination

In our reexamination we make no assumptions about pulse-to-pulse stability. We draw on three sources of information: (1) Our own numerical simulations, because we have refined theoretical models to render simulations more realistic than was feasible before, (2) our own experiments, because we recently studied a laser system which constitutes a particularly clean case of modelocking dynamics, and (3) a literature survey of experimental data on a broad range of laser types. The combined results lead us to a unified description for the output pulse width in terms of a simple formula that covers a wide range of situations including synchronously pumped OPOs. In fact, we question the concept of 'the' pulse width. In accord with [1, 6, 11] and others cited already, we come to the conclusion that over wide segments of the parameter regime there is no such thing as a well-defined pulse width. We therefore distinguish several characteristic times (all defined as FWHM): The 'bright' time τ denotes that time interval during which appreciable laser emission takes place, and the coherence time τ_c is the time scale over which the emitted light is coherent. These quantities are not normally accessible directly in an experiment. The quantity directly measured is the width $\langle\tau_a\rangle$ of an autocorrelation trace where the angled brackets remind us that normally an average over many pulses is measured. However, since the autocorrelation may be not just bell-shaped but consist of a pedestal and a coherence spike, we further distinguish $\langle\tau_{ap}\rangle$ and $\langle\tau_{ac}\rangle$ where applicable.

The calculation of the autocorrelation widths from simulated pulses presents no difficulties. To do the inverse operation requires knowledge of the pulse shape function; it also requires that the average autocorrelation shape is representative of the individual pulse autocorrelation (no fluctuations in τ). Nevertheless it is common practice to estimate τ through $\tau = C_{DEC}\langle\tau_{ap}\rangle$, where the deconvolution factor C_{DEC} occasionally is the result of a reasonable guess.

We will avoid making such assumptions. In an ideal case of a train of identical Fourier-limited bell-shaped pulses, $\langle\tau_{ap}\rangle = \langle\tau_{ac}\rangle$, and there is no coherence spike in the autocorrelation. In less clear-cut cases, we can state safely only that (i) $\tau_c \leq \tau$, (ii) τ_c equals the inverse spectral width of the pulse train, and (iii) τ_c is proportional to the width of a coherence spike in the autocorrelation, $\langle\tau_{ac}\rangle$. The goal for most people presumably is to make 'the' pulse width small. Restated, the goal should then be to minimize both τ and the shot-to-shot fluctuations simultaneously, while staying in the regime where $\langle\tau_{ap}\rangle \approx \langle\tau_{ac}\rangle$.

This paper is organized as follows. We first outline the numerical model and our experimental setup. Next, experimental data will be compared to results of our numerical computations. We will combine the influence of the most important parameters in an extended version of the description given in [18]. Then, in a survey of different laser materials we quantify the influence of the gain cross section on the minimum achievable pulse width. It will turn out that one can include even the somewhat special case of synchronously pumped OPOs. Finally, we arrive at the full equation which is the central result of this paper. It allows assessment of various factors influencing the pulse formation in a very transparent way, and, with the knowledge of certain coefficients for this laser, its performance in terms of stability and achievable pulse width can be calculated. An application is given, and limits of validity are addressed.

2 The numerical model

We implemented a numerical model of the synchronously pumped laser based on the approach of New and collaborators [4, 8, 11] that contains gain, loss, spectral filtering, and spontaneous emission noise. We augmented the model with the addition of dispersion and a realistic modeling of the tuning element. Details of the algorithm are given in the Appendix. This extended model allows a detailed comparison with experimental data. In order to simulate typical experimental procedures as realistically as possible, we performed two-parameter scans in spite of their considerably higher computational cost. This means that whenever one parameter is varied, the cavity length mismatch is continuously adjusted so as to track a required optimum situation, for example, the shortest possible average autocorrelation width $\langle\tau_{ap}\rangle$. (The choice of optimum cavity length is not trivial, and there is no complete theory to guide in the choice. We found some interesting insights on this matter which will, however, be presented elsewhere).

3 Experimental setup

The laser considered in our experiments is a NaCl:$OH^-(F_2^+)_H$ color center laser. This material lases from 1.47 to 1.7 μm, in a bandwidth of $\Delta\nu = 25$ THz, and is pumped by a Nd:YAG laser at 1.064 μm. The fluorescence lifetime was determined to be $t_1 = 150$ ns [19], and the gain cross section follows as $\sigma = 8.5 \times 10^{-17}$ cm^2. The pulse duration of the color center laser and the inclination to form satellite pulses can be significantly reduced by the use of shorter pump pulses [20], as will become clear.

To obtain compressed pulses from the Nd:YAG pump laser, we chose the concept of additive-pulse modelocking (APM; for a general overview see [21]). At $\lambda = 1.064$ μm this laser delivers nearly transform-limited pulses with a width of 6 to 10 ps and an average output power up to 5 W [22]. Using such pulses as pump pulses, the color center laser produces output pulses of down to $\langle\tau_{ap}\rangle \approx 1$ ps duration.

The color center laser is arranged in the doubly folded astigmatically compensated five-mirror setup (see Fig. 1). The color center crystal, oriented at the Brewster angle, is

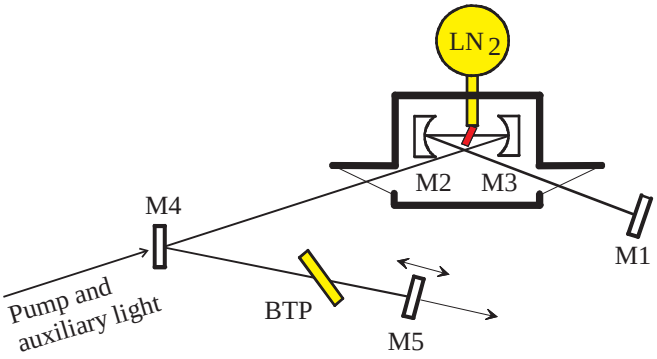

Fig. 1. Experimental setup of the NaCl:$(F_2^+)_H$ color center laser. M_i: mirrors, BTP: birefringent tuner plate, LN_2: liquid nitrogen tank

mounted on a liquid nitrogen cold finger in a vacuum chamber. It is collinearly pumped by the APM Nd:YAG laser; pump absorption in the crystal is 60%. An optical diode prevents retroreflection into the pump laser. An argon ion laser beam with about 50 mW cw auxiliary light at $\lambda = 488$ nm is collinearly adjusted with the pump beam to prevent orientational bleaching of the crystal. For tuning of the laser and for spectral filtering we use various Brewster-angled quartz birefringent tuner plates (thickness ranging from 0.325 mm to 5.2 mm). Best performance is reached with an output coupler with 22% transmission. At 6 W pump power, the laser delivers average output powers of 900 mW.

Pulse width is measured by a standard non-collinear autocorrelator. We routinely measure pulse widths by least square fit of digitized data using a Levenberg-Marquardt algorithm [23] to fit a sum of two sech^2 functions. This immediately yields $\langle\tau_{ap}\rangle$ and $\langle\tau_{ac}\rangle$ in cases when these differ, and does no harm when they do not. The same procedure is applied to numerically generated simulation data as well.

4 Towards a systematical treatment of parameter dependence

In [18] we concluded that the laser output pulse width τ can be calculated from the pump pulse width τ_p and the filter time τ_f with the expression

$$\tau = \sqrt{(C_f\tau_f)^2 + (C_p\tau_p)^2}\,, \tag{1}$$

with two empirical coefficients C_f and C_p. Additionally, there was evidence for a proportionality of the coherence time to the available bandwidth: $\tau_c = C_f\tau_f$. It implies that the pulse width is proportional to one of the characteristic times τ_f or τ_p as long as the other is small, and describes the smooth crossover when both are comparable. This expression follows quite naturally from analytical theory and is corroborated by both experiment and numerical simulations. Quite obviously, it is strongly simplified and does not hold when other factors influencing the pulse width begin to become noticeable. We will show how such further influences can be incorporated in a straightforward manner.

To avoid assumptions about the pulse shape we reformulate (1) for autocorrelation widths as

$$C_{DEC}\langle\tau_{ap}\rangle = \sqrt{(C_f\tau_f)^2 + (C_p\tau_p)^2}\,. \tag{2}$$

As already pointed out, care should be taken in calculating τ from this.

4.1 Intracavity dispersion

For state-of-the-art passively modelocked lasers with output pulses in the ten-femtosecond range, intracavity dispersion is one of the most crucial factors determining the pulse width. Here we are concerned with somewhat longer pulses so that the impact of dispersion is not quite as dominant. We can therefore restrict ourselves to a discussion of second-order dispersion $B_2 = \beta_2 l$ (l is the cavity length) [24], and neglect higher-order corrections.

In our laser, B_2 is determined mainly by the Brewster windows of the vacuum chamber, and to a lesser extent by the gain material and other components in the beam path. A realistic estimate is $B_2 = -500$ fs^2. Just how much influence this amount has on pulse shaping depends on the bandwidth of that pulse. We therefore used different combinations of tuner plates to vary the filter time and in each case measured the autocorrelation traces. The result is shown in Fig. 2 for both $\langle\tau_{ap}\rangle$ (circles) and $\langle\tau_{ac}\rangle$ (crosses). (For the solid line, see the penultimate paragraph of this section). Remarkably, $\langle\tau_{ac}\rangle$ is proportional to τ_f over the whole range. For $\langle\tau_{ap}\rangle$ the relation is more complicated. For sufficiently large τ_f, the autocorrelation shape is smooth ($\langle\tau_{ap}\rangle = \langle\tau_{ac}\rangle = \tau_a \propto \tau_f$), and we may assume that the pulse shape is stable and reasonably well known so that we can deconvolute with $C_{DEC} = 0.65$ and obtain the slope C_f. For very small τ_f, $\langle\tau_{ap}\rangle$ rises again. Even though only one tuner plate was available in this regime, the increase was reproducible and unmistakable. Let us point out that it is a well known (but badly documented) fact that judicious choice of the tuner is required for optimum performance; neither too much nor too little selectivity is desirable. The minimum of $\langle\tau_{ap}\rangle$ corresponds to the 'best' pulses because, also in this regime, $\langle\tau_{ap}\rangle$ and $\langle\tau_{ac}\rangle$ are not very different, so the autocorrelation shape is still reasonably smooth. The shortest pulse is thus characterized by $\langle\tau_{ap}\rangle = 1.6$ ps which would commonly be interpreted as $\tau = 1.0$ ps after deconvolution. There is an increase of pulse width for too much bandwidth

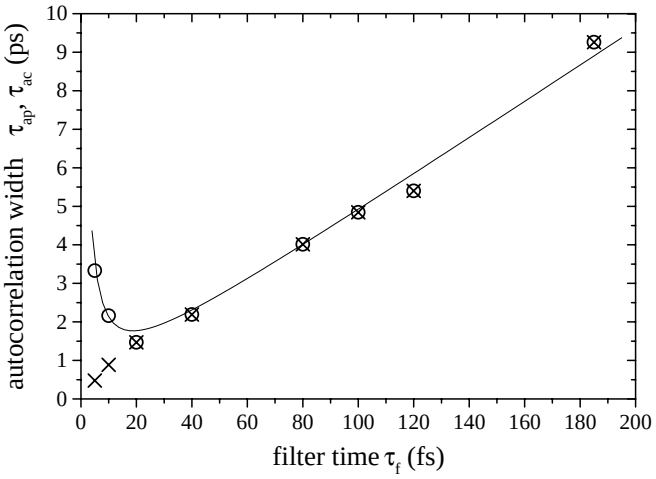

Fig. 2. Measured autocorrelation widths (circles, pedestal width τ_{ap}; crosses, coherence width τ_{ac}) as a function of filter time τ_f. The solid line is a fit of (4)

which is not described by (1) as it stands; we interpret this increase as a consequence of intracavity dispersion.

We performed numerical simulations to check whether a similar behavior is predicted by the model. Figure 3 shows the calculated pulse width (again, both pedestal width and coherence time are shown) as a function of filter time with $B_2 = -500\,\mathrm{fs}^2$. The qualitative similarity is striking. The coherence time is obviously unaffected by dispersion. The minimum pedestal width is found for the data point at $\tau_\mathrm{f} = 20\,\mathrm{fs}$, just as in the experimental data. Also, a minimum achievable pedestal width of $\langle\tau_\mathrm{ap}\rangle = 1.3\,\mathrm{ps}$ is predicted, which is in reasonable agreement with the experimental value of 1.6 ps. Again, for the solid line, see the end of this section.

In a complementary approach we varied B_2 and computed the effect on the pulse width for several birefringent tuner plates. The results are shown in Fig. 4. For a given tuner element the achieveable pulse width is constant as long as dispersion is low enough. In this region the pulse width is affected mainly by the bandwidth limiting effect of the filter and the effect of pump pulse width.

Beyond a 'cross-over' value of dispersion B_XO, $\langle\tau_\mathrm{ap}\rangle$ increases with increasing dispersion. Well beyond B_XO, $\langle\tau_\mathrm{ap}\rangle$ increases linearly with increasing dispersion with a certain slope inversely proportional to τ_f. B_XO itself increases with increasing filter time. The combination of these observations can be incorporated into (1) by the addition of a new term that is motivated by the following consideration. It is well known (see for example [24]) that (unchirped) Gaussian pulses of width τ_0 (FWHM) propagating through a dispersive medium of length z are spread out to τ_1 given by

$$\tau_1 = \sqrt{\tau_0^2 + \left(\frac{\kappa\beta_2 z}{\tau_0}\right)^2}, \tag{3}$$

with κ a pulse-shape-dependent constant of $4\ln 2$ for a Gaussian. In the case at hand, photons interact with the cavity dispersive elements for one photon lifetime which we write

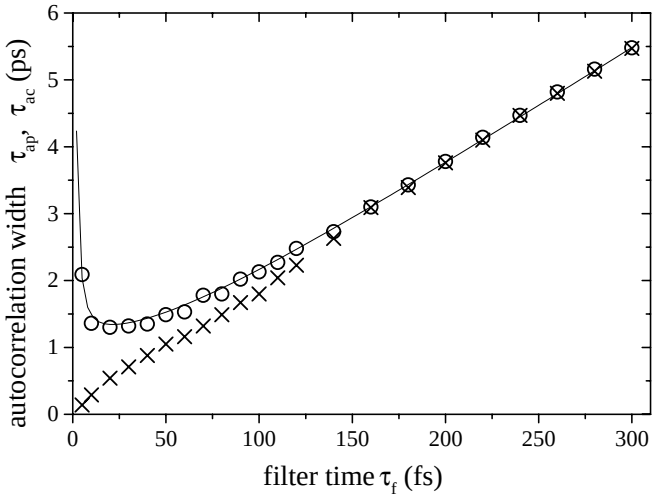

Fig. 3. Calculated autocorrelation widths (circles, pedestal width τ_ap; crosses, coherence width τ_ac) as a function of filter time τ_f under influence of intracavity dispersion. A pump pulse width of $\tau_\mathrm{p} = 10\,\mathrm{ps}$ was assumed. The solid line is a fit of (4)

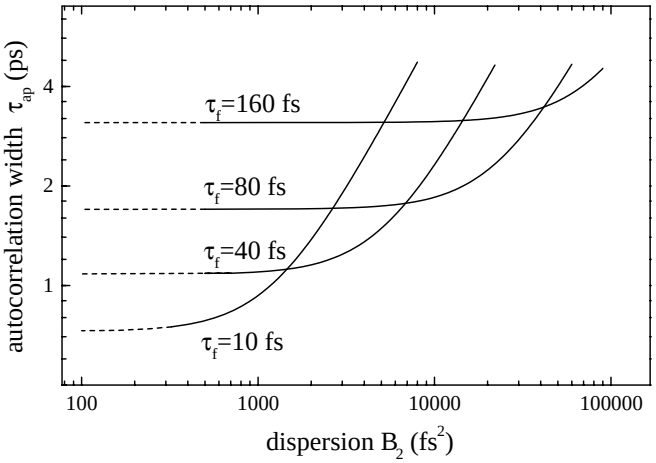

Fig. 4. Calculated autocorrelation width τ_ap as a function of intracavity dispersion B_2 for several tuner plates. A pump pulse width of $\tau_\mathrm{p} = 5\,\mathrm{ps}$ was assumed, short enough not to noticeably affect the curves shown. The solid lines are fits of (4) to the calculated data points which are not shown for clarity; scatter of points around the line is minimal. The dashed lines are continuations of the fit curves outside the range of data points

as ml with $m = 1/|\ln R|$ (R is the output coupler reflectivity). Thus we can identify $\beta_2 z = m B_2$. In the case where other contributions are small, τ_0 could be identified with $C_\mathrm{f}\tau_\mathrm{f}$ if the pulses were indeed unchirped Gaussians, which in general they are not. Therefore, a numerical correction factor (generalized time-bandwidth product) ξ is required. With a new coefficient $C_\mathrm{d} = 4\kappa^2 m\xi/C_\mathrm{f}$, this yields an extended version of (1):

$$C_\mathrm{DEC}\langle\tau_\mathrm{ap}\rangle = \sqrt{(C_\mathrm{f}\tau_\mathrm{f})^2 + (C_\mathrm{p}\tau_\mathrm{p})^2 + \left(C_\mathrm{d}\frac{B_2}{\tau_\mathrm{f}}\right)^2}. \tag{4}$$

Again, the estimation of the real pulse width $\tau = C_\mathrm{DEC}\langle\tau_\mathrm{ap}\rangle$ is only justified if $\langle\tau_\mathrm{ap}\rangle \approx \langle\tau_\mathrm{ac}\rangle$.

Equation (4) has been fitted to the data in Figs. 2 and 3 and is shown as solid lines. From Figs. 2, 3, and 4 we obtain $C_\mathrm{d} \approx 20$, 6.5, and 7, respectively. The agreement is satisfactory, considering that the fits depend on very few data points.

We argue that further factors influencing the pulse width can be incorporated into such a model. They will either contribute another term in the sum of squares, or affect one of the coefficients. In the next section we will investigate the influence of the gain cross section and extend (4) with another term.

4.2 Gain materials for synchronous pumping

The pulse-shaping mechanism in synchronously pumped lasers involves a balance between pulse shortening due to gain saturation, and pulse broadening through bandwidth limitation. Once gain modulation has formed an initial broad pulse, dynamic gain saturation takes over and, with the stronger gain in the leading part of the pulse, the trailing part is compressed. The resulting forward shift has to be compensated by cavity length mismatch. Self-consistent theories

assume that the correct mismatch is chosen and that the pulse shaping reaches a steady state in which bandwidth limitation and dispersion balance the pulse compression force.

Arguably the most important parameter that quantifies the process of gain saturation is the gain cross section σ. It determines the amount of the gain depletion caused by the laser pulse. It is closely related (in fact, inversely proportional) to the fluorescence lifetime t_1 of the gain material. The larger σ, the stronger is the saturation effect and thus the pulse shortening. In the seventies researchers believed that only media with fluorescence lifetimes shorter than the cavity round-trip time make good synchronously pumped lasers. However, it was pointed out in [25, 26] that much longer lifetimes are well suited. This fact is now the basis of synchronous pumping of many solid-state laser materials. Still, some degree of saturation is indeed necessary for efficient synchronous pumping: both pulse shortening and pulse positioning in relation to the pump pulse temporal position depend on it. If saturation becomes too weak, synchronous pumping becomes inefficient. The following data will show just where the limit is.

Table 1 shows reported pulse widths as a function of the inverse gain cross section obtained from the literature for several different gain media. Most of these were actually measured as an autocorrelation width times a deconvolution factor. We reverse the deconvolution by dividing with the deconvolution factor $C_{\mathrm{DEC}} = 0.65$; Fig. 5 shows the $\langle\tau_{\mathrm{ap}}\rangle$ data thus recovered. To display these disparate data from different sources in a meaningful way we found it helpful to group them into two categories according to the pump pulse width used. Data from most solid-state lasers tend to rise in proportion to $1/\sigma$ for not too small values of $1/\sigma$. In this regime we fit a linear function to the data. Again, on the assumption that in this regime pulses fluctuate not too much, we deconvolute to obtain C_{s}/σ with $C_{\mathrm{s}} \approx 0.40 \times 10^{-20}\,\mathrm{ps\,m^2}$. By this procedure we have avoided making any assumption about fluctuations, or the lack thereof, for the shortest pulses involved. If one extrapolates the linear trend towards large $1/\sigma$, at some point the pulse duration becomes longer than the repetition time, which is an obvious impossibility. Pulses of about a nanosecond duration mark the end of useful modelocking; note that for typical cavity round-trip times of 10 ns, only 10 modes would be coupled in such a case. Towards small $1/\sigma$ the data level out. The achievable pulse duration is 'clamped' by the effect of pump pulse width, and certainly by bandwidth limitation. As expected, the shortest pulses are obtained with dyes, and also with some color centers. For the fitted lines see the next section.

Table 1. Pulse widths and gain cross sections for different laser materials

Gain Material	$\sigma(10^{-16}\,\mathrm{cm}^2)$	τ/ps $\tau_{\mathrm{p}} \approx 80$ ps	τ/ps $\tau_{\mathrm{p}} < 20$ ps	Source
Cr:Fosterite	0.0014	260		[31]
Ti:Sapphire	0.0032	200		[32]
Cr:YAG	0.004	25		[33]
KCl:Tl	0.13	8		[25]
Na:Cl	1.7	6	0.6	[34]
KCl:$Na^+O_2^-$	1–2	6	0.9	[35]
Rhodamine 6G	1.8	3.5	0.3	
26HFB	13500	3	0.3	[17]

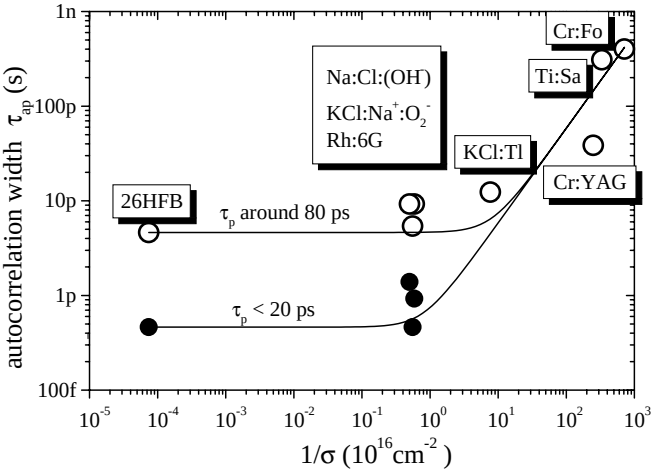

Fig. 5. Dependence of the autocorrelation width (obtained from reported pulse widths in Table 1, see text) on the gain cross section σ. The pulse widths displayed as open circles are obtained with $\tau_{\mathrm{p}} \approx 80$ ps, the solid circles belong to short pump pulses with $\tau_{\mathrm{p}} = 5$–20 ps. Solid lines: fits with (5)

As an extreme limiting case we consider gain media that have no energy storage at all, namely OPOs (for an overwiew of OPOs see for example [27]). This limit is obtained here formally by letting $t_1 \to 0$ or $1/\sigma \to 0$. This implies that best performance is reached without any cavity length mismatch. Fig. 6 and Table 2 show the dependence of the reported pulse width τ of different OPOs as a function of the pump pulse width, obtained from the literature. We distinguish cases with and without compensation of intracavity group velocity dispersion. $\langle\tau_{\mathrm{ap}}\rangle$ rises linearly for large τ_{p}; only for the non-dispersion-compensated cases does the curve level out at small τ_{p}. After deconvolution in the regime of $\langle\tau_{\mathrm{ap}}\rangle \propto \tau_{\mathrm{p}}$ we obtain $C_{\mathrm{p}} \approx 0.5$. For the fitted lines see the next section.

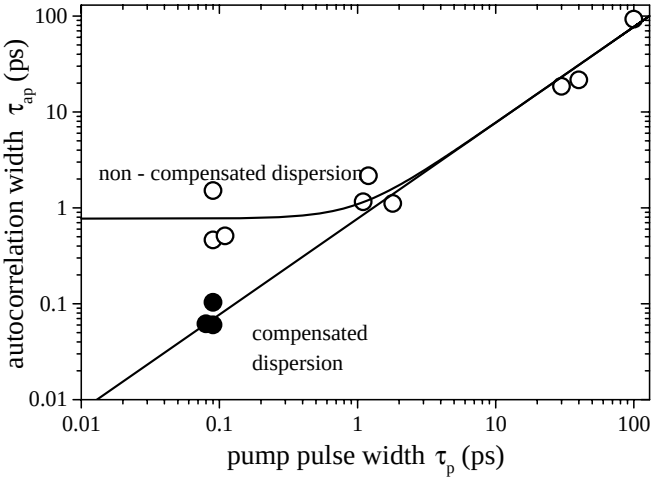

Fig. 6. Synchronously pumped OPOs: Dependence of the autocorrelation width (obtained from reported pulse widths in Table 2, see text) on the pump pulse width. Open circles: data were obtained without compensation of intracavity dispersion. Solid circles: dispersion compensated ($B_2 = 0$). Solid lines: fits with (5) with $1/\sigma = 0$, $C_{\mathrm{p}} = 0.5$, and $C_{\mathrm{d}}(B_2/\tau_{\mathrm{f}}) \approx 500$ fs

Table 2. Pulse widths and pump pulse widths for synchronously pumped optical parametric oscillators

τ_p/ps	τ/ps ($B_2 \neq 0$)	τ/ps ($B_2 = 0$)	Source
1.2	1.4		[36]
≤ 0.1	0.3	0.039	[37]
≤ 0.1	0.98	0.067	[37]
1.8	0.72		[38]
0.08		0.04	[39]
1.1	0.5–1		[40]
0.11	0.325		[41]
30–40	12–14		[42]
100	45–80		[43]

5 The unified equation

The combination of all the previous findings can be written as

$$C_{\mathrm{DEC}}\langle\tau_{\mathrm{ap}}\rangle = \sqrt{(C_{\mathrm{f}}\tau_{\mathrm{f}})^2 + (C_{\mathrm{p}}\tau_{\mathrm{p}})^2 + \left(C_{\mathrm{d}}\frac{B_2}{\tau_{\mathrm{f}}}\right)^2 + \left(C_{\mathrm{s}}\frac{1}{\sigma}\right)^2},$$
$$C_{\mathrm{DEC}}\langle\tau_{\mathrm{ac}}\rangle = C_{\mathrm{f}}\tau_{\mathrm{f}}\,. \tag{5}$$

This set of equations gives both $\langle\tau_{\mathrm{ap}}\rangle$ and the coherence time $\langle\tau_{\mathrm{ac}}\rangle$. Note that the ratio $\langle\tau_{\mathrm{ap}}\rangle/\langle\tau_{\mathrm{ac}}\rangle$ gives an indication of the quality of the pulse, or the pulse structure. Knowledge of the following laser properties is required: the filter time τ_{f}, the pump pulse width τ_{p}, the intracavity dispersion B_2, and the gain cross section σ. The model also requires four coefficients: C_{f} describes the fraction of the given bandwidth of the filter that is filled by the pulse, C_{p} the ratio of pulse width to pump pulse width, and C_{d} is the ratio of dispersive round-trip time delay across the filter bandwidth to pulse width. C_{s} is the gain cross section coefficient, and indicates the ratio of the pulse width to the characteristic time for gain depletion due to stimulated emission.

Fits of (5) are shown in Figs. 5, 6 along with the data points for various lasers and for OPOs. A very reasonable fit is obtained in either case, even though the pulse-shaping process in OPOs is not quite comparable to that in synchronously pumped lasers.

5.1 Limits and application

Of course, (5) is a simplified description of reality and does not take every conceivable factor of influence into account. The limits of validity are reached in the presence of manifest propagation effects of pump or laser pulse in the gain medium. This means that a walk-off between these pulses as commonly encountered in OPOs, or any kind of additional shaping processes, such as solitary pulse shaping or Kerr lensing, cannot be described properly. It may be argued that another fundamental limit for τ exists when all terms under the square root in (5) tend to zero, given by spontaneous emission [28]. However, due to the scarcity of available data it does not seem warranted to include this mechanism. Also, this description is only applicable in the case of optimum cavity length mismatch; let us repeat that we ensured this in our numerical work through two-parameter scans. A cavity length mismatch results in a timing mismatch and leads to very complex phenomena. In the strict sense of the term, 'synchronous pumping' would be a misnomer in such a case.

To apply (5), one first has to have knowledge of the coefficients. From the previous evaluation of widely differing lasers it seems that the values of the coefficients do not vary very much, perhaps by a factor of three. Thus, one certainly has a good initial guess even if nothing else is known about the particular laser. A few experiments will then quickly narrow down the range of values because the functional form of (5) is so apparent. We also believe that future determination of the coefficients for a couple of laser types will reveal trends that further help narrow down the initial guesses.

As an example for an application, we choose our color center laser. We already have advance knowledge about its coefficients from experiment and numerical simulation, see Table 3. As pointed out, this laser presents a particularly clean case of modelocking dynamics in the sense that effects of the pump pulse width do not swamp everything, so the other dependencies become plainly visible. Not only can one predict the minimum obtainable autocorrelation pedestal width and the most appropriate tuner plate, but also the pulse width for different tuner plates. The filter with the shortest pedestal is found from $\mathrm{d}\langle\tau_{\mathrm{ap}}\rangle/\mathrm{d}\tau_{\mathrm{f}} = 0$. We find

$$\tau_{\mathrm{f,opt}}(B_2) = \sqrt{\frac{C_{\mathrm{d}}}{C_{\mathrm{f}}}|B_2|}\,. \tag{6}$$

The resulting widths for our laser are then ($1/\sigma$ is negligible)

$$\langle\tau_{\mathrm{ap,opt}}\rangle(B_2) = \frac{1}{C_{\mathrm{DEC}}}\sqrt{2C_{\mathrm{f}}C_{\mathrm{d}}|B_2| + (C_{\mathrm{p}}\tau_{\mathrm{p}})^2}$$
$$\langle\tau_{\mathrm{ac,opt}}\rangle(B_2) = \frac{1}{C_{\mathrm{DEC}}}C_{\mathrm{f}}\tau_{\mathrm{f,opt}}\,. \tag{7}$$

Specifically, using the coefficients $C_{\mathrm{d}} = 20$, $C_{\mathrm{f}} = 30$ from Table 3 we find an optimum filter time of $\tau_{\mathrm{f,opt}} = 18$ fs. Recall that in the experiment (compare Fig. 2), $\tau_{\mathrm{f}} = 20$ fs was best. With $C_{\mathrm{p}}\tau_{\mathrm{p}} = 1$ ps the optimum autocorrelation width comes out as $\langle\tau_{\mathrm{ap,opt}}\rangle = 1.9$ ps, and the coherence time as $\langle\tau_{\mathrm{ac,opt}}\rangle = 0.8$ ps. The ratio $\langle\tau_{\mathrm{ap,opt}}\rangle/\langle\tau_{\mathrm{ac,opt}}\rangle$ gives an indication of the quality of the pulse, and in this 'optimum' parameter regime one would expect a pulse train with unsatisfactory stability. If a tuner plate of larger thickness (larger τ_{f}) were used, one would expect somewhat broader pulses of better quality. A compromise between pulse shortness on one hand,

Table 3. Complete set of parameters required for (5) for the example of our color center laser. Exp: from our experiments. Num: from the numerical model. Note that data in [14] were actually taken on a dye laser but can be used here as well

	Value	Source
τ_{p}	8 ps	measured
τ_{f}	several from 10–180 fs	from plate thickness [30]
B_2	$-500\ \mathrm{fs}^2$	from specs of components
σ	$8.5\times10^{-17}\ \mathrm{cm}^2$	[19]
C_{f}	30	Exp.
	13	Num.
C_{p}	0.02–0.07	[14–16]
	0.12	Num.
C_{d}	20	Exp.
	7	Num.
C_{s}	$0.4\times10^{-20}\ \mathrm{ps\,m}^2$	Fig. 4

and smoothness and stability on the other, is found when the $C_f\tau_f$ term is equal to the largest of the other terms in (5). This turns out to be the regime where experimentalists operated their lasers after trial and error; our description casts into a definitive form what experimentalists have felt intuitively. It is also clear that pulse quality suffers when the pump pulse width is increased, all other quantities being kept constant. Hence the particularly clean operation of our laser due to its unusually short pump pulses.

6 Conclusion

We presented our investigation of the pulse shaping mechanisms in a synchronously pumped laser. The use of picosecond pump pulses reduces the complexity of experimental performance and allows a comparison with a numerical model. The results of the simulation are in excellent agreement with experimental data. As a central result we presented a simple empirical formula which provides a unified description including the influence of pump pulse width, bandwidth filter, second-order dispersion and gain cross section on the laser pulse width. It allows an at-a-glance overview of dependencies on various parameters, information previously thought accessible only through extensive numerical modeling. Also, it allows immediate prediction of achievable pulse width, structure, and limiting factors once certain coefficients are known. Limits of validity have been indicated.

Appendix

The algorithm consists of modules for gain and loss, spontaneous emission noise, spectral filtering, dispersion, and cavity length mismatch which are now described in turn.

A.1 Gain and loss

The gain process is described by

$$V^{(\mathrm{out})}(t) = \exp\left[\frac{1}{2}(A(t) - L)\right] V^{(\mathrm{in})}(t)\,, \tag{A.1}$$

where L is the power loss coefficient. The resulting complex electric field $V^{(\mathrm{out})}(t)$ is obtained as a funtion of the incoming field $V^{(\mathrm{in})}(t)$. All sources of loss, including output coupling, are lumped into L. The power gain coefficient $A(t)$ is given by the rate equation:

$$\frac{\mathrm{d}A}{\mathrm{d}t} = P_{\mathrm{pump}}(t) - (\exp(A(t)) - 1)\left|V^{(\mathrm{in})}(t)\right|^2 - \frac{A(t)}{t_1}\,, \tag{A.2}$$

where $P_{\mathrm{pump}}(t)$ determines the pump pulse power and t_1 the fluorescence decay time [8, 29].

The last term in (A.2) will be neglected within the time window T_w due to the long upper state lifetime $t_1 \gg T_w$. Storage of inversion between successive passes through the gain medium must not be neglected, however. It is taken into account by initializing $A(t) = A(t - T_d)\exp(-T_d/t_1)$, where T_d gives the temporal delay between the two successive passes. Continuous time t is replaced by $\mathrm{i}\Delta T$, and the differential equation (A.2) is solved numerically by a 4th order predictor–corrector method [23]. In a linear cavity the pump power P_{pump} is set to zero when the pulse passes through the gain medium for the second time during every round-trip.

A.2 Spontaneous emission noise

We include noise by addition of a stochastic term S_i to the field amplitude V_i. This term is generated by the formula

$$S_i = S_{i-1}\mathrm{e}^{-\Delta T\Delta\nu} + V_{\mathrm{SE}}(t)\mathrm{e}^{i\varphi_i} \tag{A.3}$$

with random phases φ_i and noise amplitude V_{SE}. It yields Gaussian noise with a coherence bandwidth $\Delta\nu$ [11]. A realistic value for V_{SE} can be estimated from the spontaneous photon flux in the interaction volume in the laser material as $V_{\mathrm{SE}} \approx 10^{-5}\,\mathrm{W}^{1/2}$.

A.3 Spectral filtering, dispersion, and mismatch

Gain, loss and noise are directly modeled in the time domain. Spectral filtering, length mismatch and the effect of residual dispersion in the cavity are calculated in the frequency domain using the fast Fourier transform $\mathcal{F}$, $\boldsymbol{V} = \mathcal{F}(V)$:

$$\boldsymbol{V}^{(\mathrm{out})}(\omega) = T_f(\omega)\mathrm{e}^{i(T_m\omega + \frac{1}{2}B_2\omega^2)}\boldsymbol{V}^{(\mathrm{in})}(\omega) \tag{A.4}$$

with the complex spectral filter function $T_f(\omega)$, the second order dispersion B_2 and the temporal mismatch T_m. To facilitate a direct comparison to the experimental data, we implemented a detailed model of a single-stage birefringent tuner from [30].

The intracavity effects described so far can now be combined to simulate a cavity in a modular manner. For a detailed comparison of numerical calculations and experimental results we used realistic parameters for the NaCl:OH^- color center laser as a starting point. The evolution of the pulse profile in an array of 4096 complex values in a time window of $T_w \approx 100$ ps was observed for 8000 round-trips. After the transient phase had died out, the average autocorrelation function of 5000 pulses was calculated.

Acknowledgements. We gratefully acknowledge financial support from Deutsche Forschungsgemeinschaft.

References

1. H.A. Pike, M. Hercher: Appl. Phys. **41**, 4562 (1970)
2. E.W. van Stryland: Opt. Commun. **31**, 93 (1979)
3. J. Herrmann, U. Motschmann: Appl. Phys. B **27**, 27 (1982)
4. J.M. Catherall, G.H.C. New, P.M. Radmore: Opt. Lett. **7**, 319 (1982)
5. G.H.C. New, J.M. Catherall: Opt. Commun. **50**, 111 (1984)
6. D.B. McDonald, J.L. Rossel, G.R. Fleming: IEEE Quantum Electron. QE **17**, 1134 (1981)
7. U. Stamm: Appl. Phys. B **45**, 101 (1988)
8. S. Kelly, G.H.C. New, D. Wood: Appl. Phys. B **47**, 349 (1988)
9. W. Forysiak, J.V. Moloney: Phys. Rev. A **45**, 3275 (1992)
10. W. Forysiak, J.V. Moloney: Phys. Rev. A **45**, 8110 (1992)
11. J.M. Catherall, G.H.C. New: IEEE Quantum Electron. QE **22**, 1593 (1986)
12. C.P. Ausschnitt, R.K. Jain: Appl. Phys. Lett. **32**, 727 (1978)

13. C.P. Ausschnitt, R.K. Jain, J.P. Heritage: IEEE Quantum Electron. QE **15**, 912 (1979)
14. A.M. Johnson, W.M. Simpson: J. Opt. Soc. Am. B **2**, 619 (1985)
15. T. Kurobori, A. Nebel, R. Beigang, H. Welling: Opt. Commun. **73**, 365 (1989)
16. K. Möllmann, M. Schrempel, B.-K. Yu, W. Gellermann: Opt. Lett. **19**, 960 (1994)
17. P. Beaud, B. Zysset, A.P. Schwarzenbach, H.P. Weber: Opt. Lett. **11**, 24 (1986)
18. F. Mitschke, U. Morgner, G. Steinmeyer: Appl. Phys. B **62**, 375 (1996)
19. J.F. Pinto, E. Georgiou, C.R. Pollock: Opt. Lett. **11**, 519 (1986)
20. G. Steinmeyer, U. Morgner, M. Ostermeyer, F. Mitschke, H. Welling: Opt. Lett. **18**, 1544 (1993)
21. F. Mitschke, G. Steinmeyer, H. Welling: In *Frontiers in Nonlinear Optics* (IOP Publishing, Bristol, 1993), p. 240
22. F. Mitschke, G. Steinmeyer, M. Ostermeyer, C. Fallnich, H. Welling: Appl. Phys. B **56**, 335 (1993)
23. W.H. Press, S.A. Teukolsky, W.T. Vetterling, B.P. Flannery: *Numerical Recipes in C* (Cambridge University Press, New York, 1992)
24. G.P. Agrawal: *Nonlinear Fiber Optics* (Academic Press, San Diego, 1995)
25. L.F. Mollenauer, N.D. Vieira, L. Szeto: Opt. Lett. **7**, 414 (1982)
26. Z.A. Yasa: Opt. Lett. **8**, 277 (1983)
27. H.M. van Driel: Appl. Phys. B **60**, 411 (1995)
28. V. Petrov, W. Rudolph, U. Stamm, B. Wilhelmi: Phys. Rev. A **40**, 1474 (1989)
29. A.E. Siegman: *Lasers* (University Science Books, Mill Valley 1986)
30. G. Phillipps, P. Hinske, W. Demtröder, K. Möllmann, R. Beigang: Appl. Phys. B **47**, 127 (1988)
31. A. Seas, V. Petricevic, R.R. Alfano: Opt. Lett. **16**, 1668 (1991)
32. Ch. Spielmann, F. Krausz, T. Brabec, E. Wintner, A.J. Schmidt: Opt. Lett. **16**, 1180 (1991)
33. P.J. Conlon, Y.P. Tong, P.M.W. French, J.R. Taylor, A.V. Shestakov: Opt. Lett. **19**, 1468 (1994)
34. T. Kurobori, K. Aoki, T. Segawa, N. Takeuchi: Jpn. Appl. Phys. **29**, 1951 (1990)
35. K. Möllmann, F. Mitschke, W. Gellermann: Opt. Commun. **83**, 177 (1991)
36. C. Fallnich, B. Ruffing, T. Herrmann, A. Nebel, R. Beigang, R. Wallenstein: Appl. Phys. B **60**, 427 (1995)
37. D.T. Reid, M. Ebrahimzadeh, W. Sibbett: Appl. Phys. B **60**, 437 (1995)
38. M. Ebrahimzadeh, S. French, W. Sibbett: Appl. Phys. B **60**, 443 (1995)
39. J.D. Kafka, M.L. Watts, J.W. Pieterse, R.L. Herbst: Appl. Phys. B **60**, 449 (1995)
40. A. Nebel, H. Frost, R. Beigang, R. Wallenstein: Appl. Phys. B **60**, 453 (1995)
41. T.F. Albrecht, J.H.H. Sandmann, J. Feldmann, W. Stolz, E.O. Göbel, H. Hillmer, R. Lösch, W. Schlapp: Appl. Phys. B **60**, 459 (1995)
42. C. Grässer, D. Wang, R. Beigang, R. Wallenstein: J. Opt. Soc. Am. B **10**, 2218 (1993)
43. E.C. Cheung, K. Koch, G.T. Moore: Opt. Lett. **19**, 631 (1994)